Electronic Supplementary Material (ESI) for Journal of Materials Chemistry A.

Supporting Information

Enhancing Surface Oxygen Retention through Theory-guided Doping Selection in layered Ni-rich Cathodes for Next-generation Lithium-ion Batteries

Jianli Cheng,[†,‡] Linqin Mu,[¶] Chunyang Wang,[§] Zhijie Yang,[¶] Huolin L. Xin,[§] Feng Lin,[¶] and Kristin A. Persson[*,†,‡]

†*Department of Materials Science and Engineering, University of California, Berkeley, CA 94720-1760, USA*

‡*Energy Storage and Distributed Resources Division, Lawrence Berkeley National Laboratory, Berkeley CA 94720, USA*

¶*Department of Chemistry, Virginia Tech, Blacksburg, Virginia 24061, United States*

§*Department of Physics and Astronomy, University of California, Irvine, CA 92697, USA*

E-mail: kapersson@lbl.gov

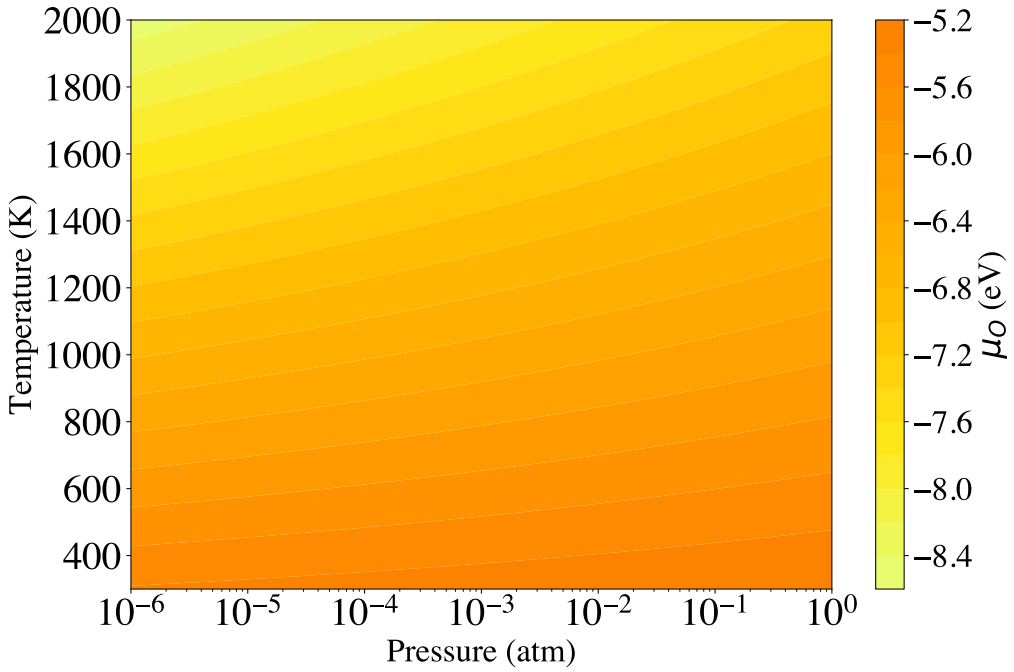

Figure S1: Calculated μ_O as a function of T and P

Oxygen Chemical Potential Dependence of Temperature and Pressure

Oxygen chemical potential (μ_O) is related to the sample preparation environment, and can be further expressed as: $\mu_O(T,P) = \mu_O + \Delta\mu_O(T,P)$. For the elemental reference μ_O, we choose the total energy of the isolated ground state O_2 molecule. At temperature T_0=298 K and pressure P_0=1 atm, O_2 standard enthalpy H_0=8.7 KJ mol^{-1} and entropy S_0=205 J mol^{-1} K^{-1}.[1] The relative oxygen chemical potential $\Delta\mu_O$ at temperature T and pressure P_0 can be expressed as:[2]

$$\Delta\mu_O(T,P_0) = \frac{1}{2}\{[H_0 + \Delta H(T)] - T[S_0 + \Delta S(T)]\} \tag{1}$$

where $\Delta H(T) = C_P(T - T_0)$ and $\Delta S(T) = C_P ln(T/T_0)$. Applying the ideal gas law for $T \geq 298$ K, the constant-pressure heat capacity C_P per diatomic molecule is $C_P = 3.5k_B$. For pressure other than P_0=1 atm, $\mu_O(T,P) = \mu_O(T,P_0) + \frac{1}{2}k_B T ln(P/P_0)$.[3] As a result, we are able to relate oxygen chemical potential with the corresponding temperature and pressure. Fig. S1 illustrates the change of μ_O as a function of T and P.

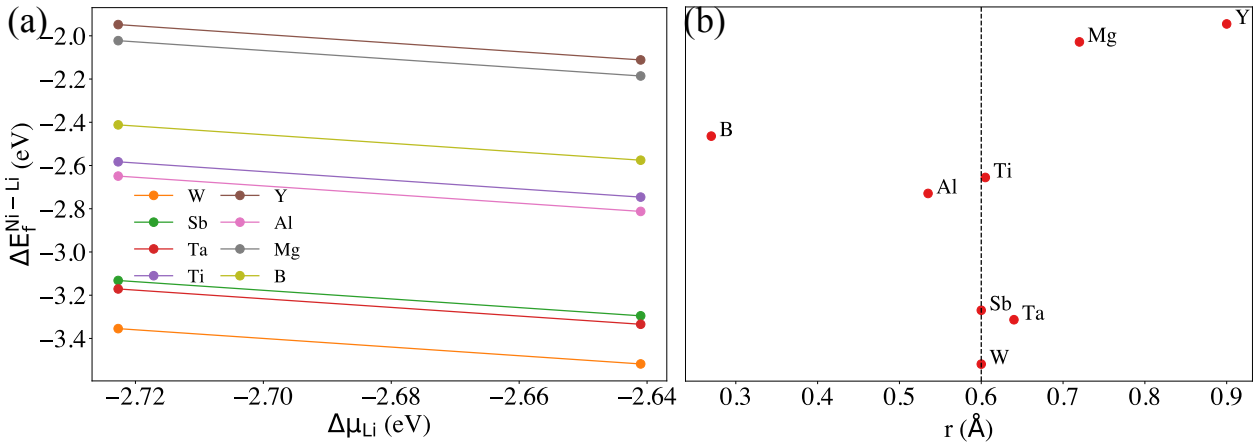

Figure S2: (a) Calculated doping formation energy difference (ΔE_f^{Ni-Li}) between doping at Ni- and Li-site of doped-$LiNiO_2$ as a function of relative lithium chemical potential ($\Delta\mu_{Li}$). (b) Doping formation energy difference of the dopants as a function of their corresponding ionic radii.[4] The vertical dashed line represents the ionic radius of Ni^{3+}

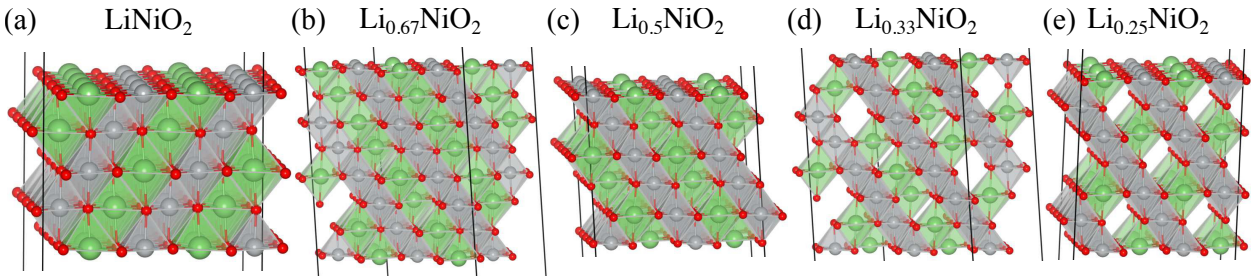

Figure S3: The configurations of $Li_{1-x}NiO_2$ slab models with (104) surface facet with (a) x=0, (b) x=0.33, (c) x=0.5, (d) x=0.67, (e) x=0.75. (Color code: green for Li atom, grey for Ni atom and red for O atom).

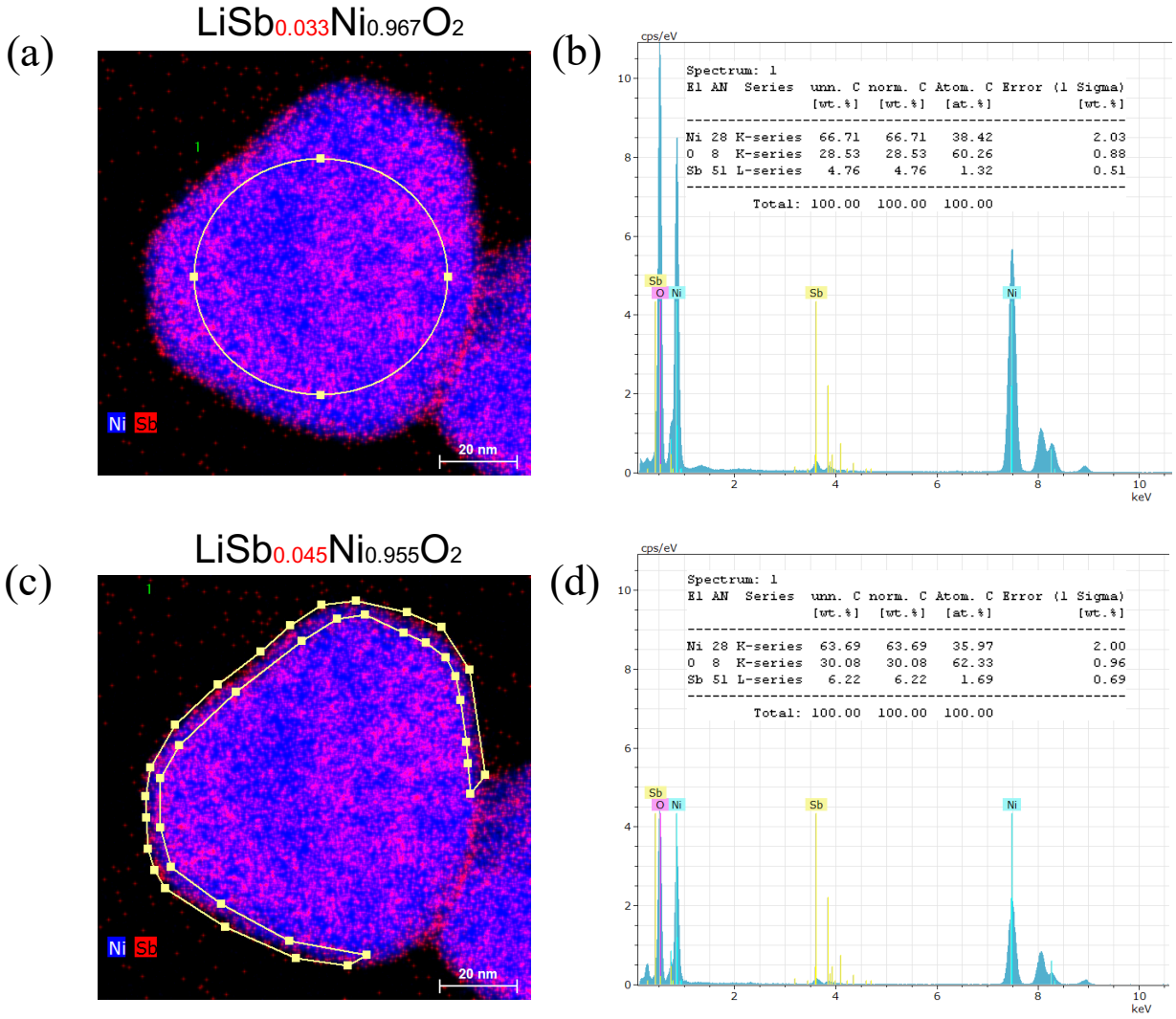

Figure S4: (a) Overlapped EDS map of Sb and Ni in doped-$LiNiO_2$. (b) Integrated EDS spectrum from the circled region (interior of the particle) and the compositional quantification of O, Ni and Sb. (c,d) Integrated EDS spectrum from the selected region (surface of the particle) in (c) and quantification of the compositions of O, Ni and Sb. The ratios of Sb/(Sb+Ni) in the interior region and surface region are determined as 3.3 and 4.5 at.%, respectively.

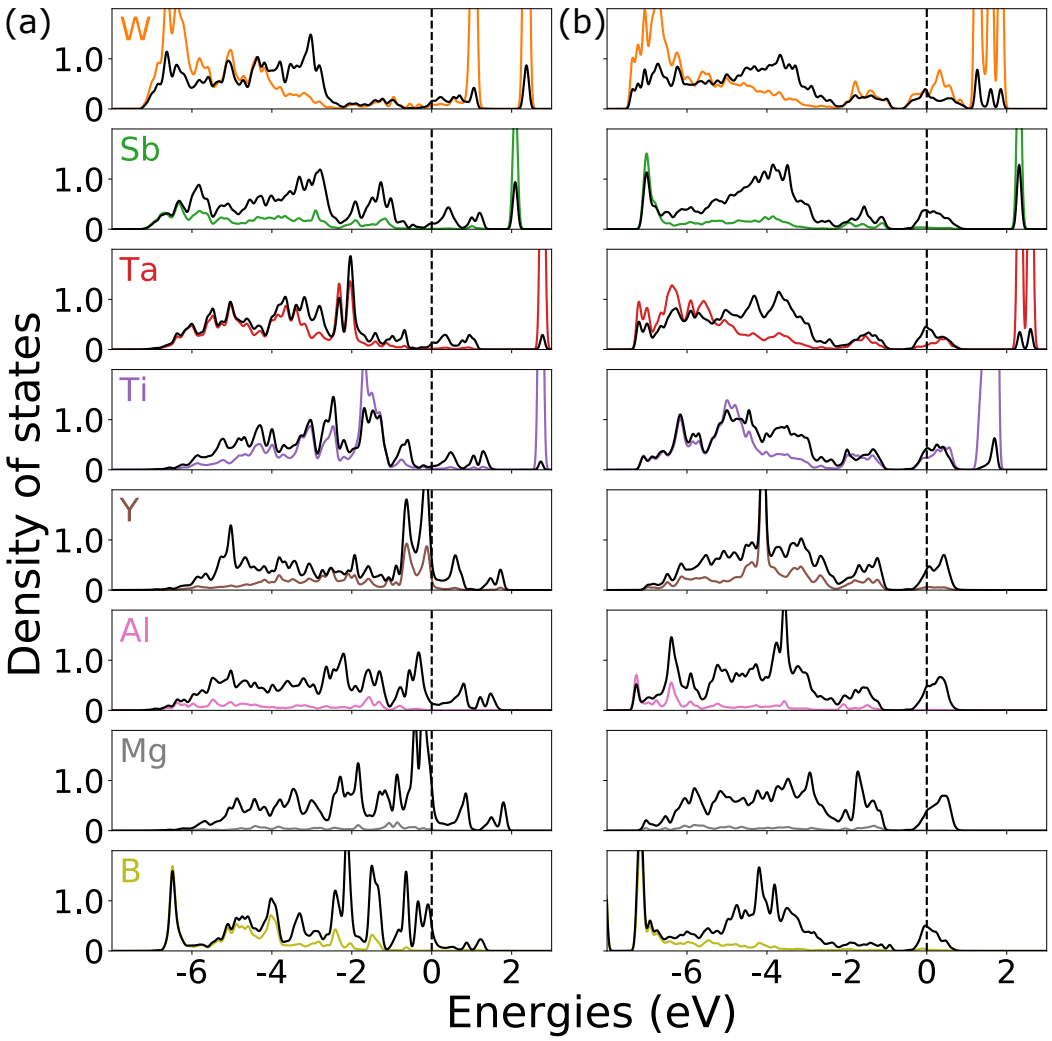

Figure S5: Calculated partial density of states (PDOS) for dopants and neighboring oxygen atoms at the surface (a) and the bulk layer (b) in doped-$LiNiO_2$. Black solid lines represent oxygen PDOS.

References

(1) Haynes, W. M. CRC Handbook Chemistry and Physics. *CRC Press* **2016**,

(2) Osorio-Guillen, J.; Lany, S.; Barabash, S. V.; Zunger, A. Magnetism without magnetic ions: percolation, exchange, and formation energies of magnetism-promoting intrinsic defects in CaO. *Phys Rev Lett* **2006**, *96*, 107203.

(3) Reuter, K.; Scheffler, M. Composition, structure, and stability ofRuO2(110)as a function of oxygen pressure. *Physical Review B* **2001**, *65*.

(4) Shannon, R. Revised effective ionic radii and systematic studies of interatomic distances in halides and chalcogenides. *Acta Crystallographica Section A* **1976**, *32*, 751–767.